
Paleogeographic significance of unknown hyperextended continental crust in South Atlantic conjugated margin

Teixeira C.D. ^{1,*}, Girelli T.J. ¹, Serratt H. ^{1,2,3}, Oliveira H.O.S. ¹, Cruz M.F. ¹, Conti B. ⁴, Rodriguez P. ⁴, Chemale F. ¹

¹ Geology and Geophysics Research Group – NGA, Universidade do Vale do Rio do Sinos, São Leopoldo, RS, Brazil

² Geology Graduate Program, Universidade de Brasília, Distrito Federal, Brazil

³ UMR CNRS-IFREMER-CNRS-UBS 6538 Geo-Ocean, IUEM, Université de Bretagne Occidentale, France

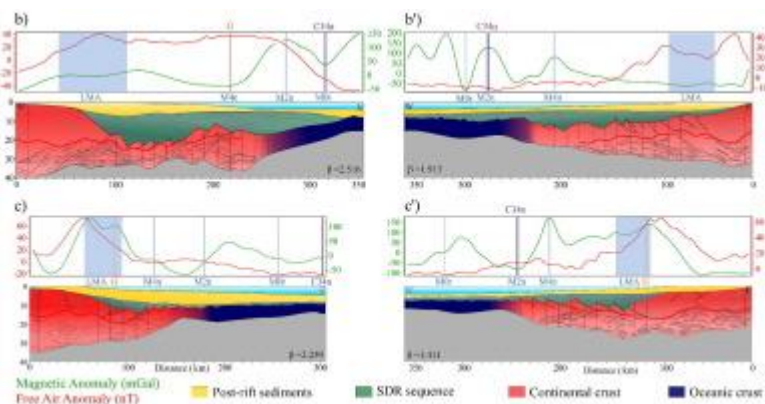
⁴ Exploration & Production, ANCAP, Montevideo, Uruguay

* Corresponding author : C. D. Teixeira, email address : claudiadx@gmail.com

Abstract :

The paleogeographic reconstruction of fragmented and dispersed continents often poses a challenge due to the lack of information regarding the nature of that extend beneath passive margin basins. To define the width of the continental crust beneath passive margin basins and its implications for paleogeographic reconstruction of conjugate continental margins, this study investigates the architecture of the stretched continental crust of the southern South Atlantic conjugate margin. The investigated region encompasses South Africa, Namibia, southern Brazil, and Uruguay, which were formed during the Mesozoic rifting of SW Gondwana. Employing a multi-tool approach combining seismic interpretation, gravity, magnetometry, and U-Pb isotopic data, the research aims to quantify the extension of stretched continental crust and its implications for plate reconstructions. The study reveals that the restored stretched crust spans at least 150 km, emphasizing the significance of considering connections between both margins for realistic paleogeographic reconstructions. Furthermore, the distinct U-Pb zircon age distribution patterns between SW Africa and SE South America reinforce the lack of direct connections despite their Gondwanan origin. The missing link estimated in this study is around 150 km, comparable in size to major mountain ranges such as the Andean or Urals. This work sheds light on critical aspects of Earth's dynamic crustal evolution and emphasizes the need for comprehensive reconstructions considering stretched and eroded crust in the South Atlantic conjugate margin

Graphical abstract



Highlights

- ▶ A multi-tool approach reveals at least 150 km of hyperextended continental crust.
- ▶ This study highlights the significance of stretching in reconstruction studies.
- ▶ Distinct U-Pb zircon age distribution patterns reinforce the lack of direct connections.
- ▶ New insights on the dynamics of hyperextended crust.
- ▶ A significant portion of the Brazilian/Pan-African orogenic belt is hidden beneath passive margin basins.

Keywords : Hyperextended continental crust, Reconstruction, South Atlantic Ocean, Passive margin, Gondwana

35

1. Introduction

36

37

38

Throughout the last decades, several studies were carried out on rifted continental margins and hyperextended continental crust in the passive margin, providing knowledge on this topic in the different magma-poor, magma-rich, and sediment-rich passive margins (e.g.,

39 Peron-Pinvidic et al., 2013; Doré and Lundin, 2015; Lei et al., 2020). Many of these studies
40 have specifically focused on the extension at rifted continental margins in association with the
41 South Atlantic opening, offering valuable insights into the tectonic evolution of this region
42 (e.g., Rabinowitz and Labrecque, 1979; Moulin et al., 2010; Granot and Dymant, 2015;
43 Chauvet et al., 2021). Although geoscientists understand this process well, accurately
44 determining its impact on paleo-plate reconstructions remains challenging. The challenge lies
45 mainly in precisely characterizing the amount of continental crust stretched. It occurs due to
46 the sedimentary and volcanic package cover over the stretched continental crust (Mutter et al.,
47 1982; Sutra et al., 2013; Nirrengarten et al., 2018). To address this, gravimetry, magnetometry,
48 and seismic data play a crucial role in providing information essential to understanding the
49 dynamic processes shaping the Earth's crust. This information helps create realistic
50 paleogeographic reconstruction models and define subsurface geological structures in
51 conjugate margins separated by the formation of oceans. Regarding this scenario, the South
52 Atlantic Conjugate Margin (SACM), comprising South Africa, Namibia, southernmost Brazil,
53 and Uruguay, provides an ideal opportunity to better understand the effects of stretched crust
54 on paleo plate reconstruction (Fig. 1).

55 The South Atlantic conjugate margins exhibit significant asymmetry, with uneven
56 extension documented in this region and observations showing significant crustal architecture
57 asymmetry, SDR type distribution, and total volume of SDR (Chauvet et al., 2021). This
58 asymmetry is a crucial consideration in understanding the evolution of the margins and the
59 distribution of stretched continental crust. Quantifying the extent of asymmetric extension is
60 challenging, but it has significant implications for plate reconstructions and understanding the
61 geological history of the region.

62 Our study aims to quantify the extension of continental crust stretched during the rifting
63 process of SW Gondwana and better understand the impact of this in plate reconstruction
64 models. We combined regional seismic interpretations, gravity, and magnetometry data from
65 the South Atlantic Ocean and onshore emerged margins. Additionally, focusing on evaluating
66 the impact of the lack of geological structures between both sides, we did a comparative
67 analysis based on U-Pb isotopic data from zircons grains in emerged margins. Based on the
68 results obtained by this multiple-tool approach, we could identify that the amount of stretched
69 crust is at least 150 km. Furthermore, the U-Pb data reinforce the lack of direct correlation
70 between these margins, which would be lost in this stretched interval. This study sheds light
71 on three questions: (i) The absence of direct structural correlation between structures in SW
72 Africa and SE South America; (ii) The presence of hyperextended crust on volcanic passive
73 and sedimentary rich margins; (iii) It is critical to consider the structural ties between both
74 margins to discuss the Precambrian tectonic evolution models.

75 **2. Geological settings**

76 The Gondwana history is a common point in the geological history of Africa and South
77 America. The formation of the Gondwana paleo continent took place during the
78 Neoproterozoic era (Veevers, 2004). Our study area (Fig. 1) was affected by the subduction of
79 the Adamastor Ocean during the Gondwana formation (Veevers, 2004; Caxito et al., 2022).
80 This significant event is recorded in the Pan-African/Brasiliano orogenic belts of South
81 America and Africa (e.g., Chemale et al., 2012). This orogenic cycle profoundly influences the
82 NE–SW structures in the southernmost regions of Brazil and Uruguay margins (Fernandes et
83 al., 1994).

84 Meanwhile, consensus regarding the subduction direction remains elusive (Basei, 2000;
85 Chemale, 2000), as does the paleogeographic reconstruction of the various orogenic belts from
86 the Neoproterozoic to the Eopaleozoic. This uncertainty is primarily due to a lack of
87 petrotectonic assemblages and more complete rock associations (e.g., juvenile arcs and
88 ophiolites). One of the key areas of interest is the underlying continental crust of the passive
89 margin basin, about which we have little information regarding the nature of these rocks. The
90 local process of Gondwana's break-up unfolded within these structures, as observed by the
91 margin, and aligned parallel these structures in southernmost Brazil and Uruguay. Even the
92 emplacement of syn-rift magmatism during the rifting of the SW Gondwana is intricately
93 linked to these pre-existing structures, which should be considered as the primary magmatic
94 conduit of the SDR (Seaward Dipping Reflectors; Fig. 2; Chauvet et al., 2021; Serratt et al.,
95 2022).

96 The studied sector is formed of a Precambrian basement that comprises in the eastern
97 side the Kaoko, Damara, and Gariiep belts (Begg et al., 2009; Frimmel, 2009; Haas et al., 2021)
98 and in the western sector, the Dom Feliciano Belt (Basei, 2000; Chemale, 2000). The Damara
99 Belt is associated with the docking between the Congo and Kalahari cratons, with an NE–SW
100 direction and subduction towards the north under the Congo Craton (Prave, 1996; Passchier et
101 al., 2002). The Kaoko Belt is characterized by dominantly E–NE-oriented structures and
102 subdivided into eastern, central, western, and southern zones (Miller and Grote, 1988; Porada,
103 1989). The Gariiep Belt is related to a part of the larger network of Pan-African/Brasiliano
104 orogenic belts in SW-Gondwana (Frimmel, 2009). In turn, the NE–SW Dom Feliciano Belt
105 records the docking between Rio de La Plata and Kalahari cratons with main structures-
106 oriented NE–SW (Hartman et al., 2007; Phillip et al., 2016; Basei et al., 2018; Will et al., 2020).
107 These Precambrian belts were partially covered by Phanerozoic sedimentary basins, such as
108 Paraná and Cape-Karoo (e.g., Milani et al., 2008).

109 This supercontinent, formed during the Neoproterozoic and later incorporated in the
110 Pangaea supercontinent, was fragmented throughout the Cretaceous, giving rise to the
111 conjugate margin of southwestern Africa and southeastern South America. The onset of rifting
112 was marked by extensive magmatism of the Paraná-Etendeka Large Igneous Province (LIP),
113 approximately 134 million years ago, associated with the Tristan da Cunha plume (Gomes and
114 Vasconcelos., 2021). This fragmentation process propagated from the south to the north,
115 forming the Walvis Ridge at around 127–133 Ma (Macdonald et al., 2003; Torsvik et al., 2009;
116 Heine et al., 2013), recording the movement of the African Plate over the mantle hot spot during
117 the separation of the African and South American continents and the formation of the South
118 Atlantic Ocean. This LIP magmatism was preceded by the SDR magmatism, recorded in both
119 margins, and that characterizes both margins as Volcanic Passive Margins (Chauvet et al.,
120 2021; Serratt et al., 2022). The rift and drift sedimentation in the studied sector originated in
121 the offshore basins of Orange, Luderitz, and Walvis in Namibia and Pelotas and Punta del Este
122 in Brazil and Uruguay.

123 **3. Methods and materials**

124 The accurate determination of lithospheric stretching requires a comprehensive, multi-
125 tool approach. Our study employed seismic interpretation as a robust tool for measuring
126 lithospheric stretching, which provided detailed insights into subsurface structures.
127 Additionally, we complemented this approach with gravity and magnetic profiles. The
128 integration of potential data delineated the boundaries of lithospheric stretching, offering a
129 robust understanding of the geophysical characteristics that result from the stretching

130 processes. Lastly, we compared the analysis of U-Pb isotopic data from zircons grains in the
131 emerged margins.

132 **3.1. Lithosphere stretching**

133 The methodology employed for calculating lithosphere stretching encompasses seismic
134 line profile interpretation previously published by Chauvet et al. (2021), crustal thickness
135 estimation, and the calculation of stretching factors, utilizing the concept of "half-space
136 stretching" to ascertain the lithosphere stretching factor (β ; McKenzie, 1978), identifying the
137 crust limits, followed by the determination of both non-extended and stretched crustal
138 thicknesses. The stretched crustal thickness is measured from the base of the SDR layer to the
139 Moho boundary. The non-extended thickness was measured as the entirety of the crustal
140 thickness extending inland from the crustal necking. Thickness measurements are taken at
141 various points along seismic profiles. Subsequently, the stretching factor (β) is estimated by
142 considering the thickness ratio between the non-extended and post-extension transition crust
143 (McKenzie, 1978).

144 To precisely delineate the regions of lithospheric stretching in each seismic profile, we
145 conducted correlation analyses with magnetic and gravity responses using the Free Air
146 anomaly grid from Sandwell et al. (2014) and the Magnetic Anomaly grid from Maus et al.
147 (2009). This correlation allowed to match previously published magnetic anomalies by
148 Rabinowitz and Labrecque (1979; G, M3, M0) and Moulin et al. (2010; LMA, M4, M2, M0)
149 to delineate with more precision the regions with lithospheric stretching.

150 Our restoration of the stretched continental crust assumes that volcanic dykes comprise
151 50% of the total volume, based on observations from other volcanic passive margins (Myers,
152 1980) and supported by seismic, potential, drilling data from the region (Harkin et al., 2020;
153 Serratt et al., 2022). As shown in Fig. 2, the drilling data reveals that the stretched crust consists
154 of volcanic rocks interlayered with pyroclastic and/or sedimentary rocks. The 50% here
155 assumed is the maximum estimation in the Myers study, so based on this, we used this number
156 to have the less extrapolated value. The presence of extensive volcanic dykes and interlayered
157 volcanic and sedimentary rocks can obscure the underlying continental crust, making it difficult
158 to assess its characteristics.

159 **3.2. Isotope record**

160 The use of zircon databases combined with geological data is a powerful tool for
161 estimating the cumulative growth of continental crust and discriminating the source area of
162 different geological terranes. To compare the major source rocks for the onshore basement
163 rocks of the studied conjugate passive margin, we use the U-Pb zircon databases of southern
164 South America and SW Africa. For the South American margin, we compiled 16,692
165 individual analyses over a hundred studies conducted since 1985 in southern Brazil and
166 Uruguay shields. Similarly, a comprehensive dataset of 16,005 individual analyses from SW
167 Africa, encompassing Pan-African Belts and cratonic areas, was compiled by Puetz (2018) and
168 Puetz et al. (2021). From these data, 7953 in southern Brazil and Uruguay and 2187 in Namibia
169 correspond to zircons in igneous rocks.

170 **3.3. Gravimetric and magnetic data**

171 Gravity and magnetic anomalies provide constraints on the structure of the Earth's crust.
172 It can help to detail their structural connections by integrating these data into the reconstruction.

173 We reconstruct the pre-to-early stretching process before oceanic crust formation at 150 Ma
174 using GPlates based on the rotational poles from Müller et al. (2019). We analyze the marine
175 gravity and magnetic anomalies preserved on the South American and African plates using the
176 Earth Magnetic Anomaly Model (Maus et al., 2009) and the Satellite Free-air Gravity Anomaly
177 data (Sandwell et al., 2014).

178 **4. Results**

179 The connections between East South America and West African margins have been
180 known since du Toit (1927), and hundreds of research studies improved this knowledge
181 throughout the last century. Nevertheless, despite these efforts, certain geological gaps remain
182 open. Since the development of GPlates Software (Müller et al., 2018), the representation of
183 plate tectonic positions and motions has been substantially improved. In South America and
184 Africa, the stretching process begins at 155 Ma in the southernmost portion, southward of the
185 study area (Jokat et al., 2003). Using this as a time constraint and based on the rotational poles
186 from Müller et al. (2019), we reconstructed the pre-to-early stretching process before oceanic
187 crust formation at 150 Ma (Fig. 3). The reconstruction carried out incorporating the magnetic
188 and gravimetric data to the block models allowed us to establish the lack of a clear connection
189 between structures in both margins. The lack of a direct link raises questions about the extent
190 of the crustal loss during the break-up.

191 The clues for the lack of a direct connection between these two continents begin to be
192 clear when we interpret the seismic lines from both margins. Through the regional seismic lines
193 in the North Pelotas Basin (Fig. 3a), it is possible to observe the SDR's below the drift
194 sedimentary rocks, represented in detail by the basalt drill core on the right and above the
195 stretched continental crust. A similar pattern can be observed in the Luderitz Basin (conjugate
196 margin, Fig. 3b). So, in the southern South Atlantic Ocean, a hyperextend continental crust
197 occurs below a thick volcanic and sedimentary package of Cretaceous to recent rocks (Fig. 3),
198 as already described by Chauvet et al. (2021). However, determining oceanic and continental
199 crust boundaries in volcanic passive margins is challenging, and it is key information for
200 continental crust restoration. Knowing this, we used previously published magnetic anomalies
201 M2 and M4 (Rabinowitz and Labrecque, 1979; Moulin et al., 2010) to help define these
202 boundaries. The first opening stage occurred between chrons M4 and M2, and the magnetic
203 anomaly M2 denotes early oceanic crust formation (Koopmann et al., 2014; Fig. 3). This initial
204 stage was characterized by basement flexure, proximal SDR deposition, and high-amplitude
205 magnetic anomalies (Serratt et al., 2022). Based on this, we could measure the continental crust
206 that spans up to 450 km beneath the volcanic and sedimentary deposits of the passive margins.

207 Using this information on continental crust offshore extension, we quantified the pre-
208 drift margin width by the calculated stretching factor. We divided the margin into two main
209 domains: Unstretched Continental Crust (UCC) and Stretched Continental Crust (SCC) (Fig. 3
210 and Table 1). For the present study, we attributed the (β) as close to one for the unstretched
211 sector, and the information about the extension of this crust is important in quantifying the total
212 crustal gap between the onshore portions. In turn, the stretched sector (SCC) was also measured
213 because it is important to understand the amount of stretched crust that can be restored (Table
214 1). The restored crust process of stretched crust considered the estimated volcanic dikes (up to
215 50%; see discussions) and the stretching factor (Table 1). Four sections were used for the
216 present study: two on the South American margin (Fig. 3b and c) and two on the SW Africa
217 margin (Fig. 3b' and c'). These sections show a stretched continental crust covered by the
218 passive margin sedimentary rocks and SDR basalts. The section b, situated in the Pelotas Basin

219 (PB), displays a stretched continental crust of 177.04 km, while the section of the conjugate
 220 margin (Fig. 3b') in the Walvis Basin (WB) has an estimated stretched crust of 187.06 km.
 221 Considering the continental crust extension, the conjugate b–b' the crustal stretching factor (β)
 222 in the South American margin is between 2.52 in the north Pelotas Basin and 1.91 in the Walvis
 223 Basin. The restored for each margin is 74.68 (PB) and 95.72 (LB; Table 1), and the final gap
 224 results from the sum of unstretched and restored crust for each side reaching in b–b' the section
 225 between northern Pelotas and Walvis basins with 170.40 km (see section b–b' in Fig. 3a).

226 The conjugate c–c' profiles exhibit a stretched continental crust (SCC) of 110.90 km for
 227 the Punta del Este Basin profile (PLB; Fig. 3c) and 229.57 km for the Lüderitz Basin profile
 228 (LB; Fig. 3c'). The values on the eastern Atlantic margin are from 1.91 in the Walvis Basin and
 229 1.41 in the Lüderitz Basin. The restored margins width range between 141.19 km and 123.37
 230 km, respectively, in the Punta del Este (Fig. 3c) and Lüderitz (Fig. 3c') basins (Table 1). The
 231 final gap results from the sum of unstretched and restored crust for each side reaching in b–b'
 232 the section between Punta del Este and Lüderitz basins with 267.56 km of gap, taking into
 233 account the 50% of suppression in the stretched crust.

234 We compare the tectonic similarities between these regions by analyzing the
 235 distribution of zircon age patterns in the onshore rocks from the conjugate margins of southern
 236 South America and SW Africa. A compilation of 16,592 zircon grains from Southeast South
 237 America and 16,005 from southwestern Africa offers a comprehensive overview of the main
 238 crustal cycles in both areas (Fig. 4). This analysis allows us to distinguish the age pattern
 239 distribution along the continental onshore margins of southern South America and SW Africa.
 240 The age spectra in Southeast South America (in blue, Fig. 4) are distributed in three main peaks.
 241 Two of these correspond to Neoproterozoic events related to the Dom Feliciano Belt: (I) the
 242 most important one corresponds to the Ediacaran–Cryogenian interval related to the collisional
 243 stage; (II) the second one corresponds to the Tonian period, related to the arc stage; the last one
 244 (III) corresponds to the Paleoproterozoic, Rhyacian–Siderian period, related to the accretion of
 245 Rio de La Plata Craton units. These peaks are similarly identified in the igneous rocks of the
 246 region. In turn, southwestern Africa (in red, Fig. 4) presents three major peaks: (i) at the
 247 Mesoproterozoic, Stenian to Ectasian period, (ii) at the Paleoproterozoic Statherian to Orosirian
 248 period, and (iii) Meso to Paleo-Archean. Regarding the Namibian igneous rocks, the main peak
 249 is restricted to the Stenian to Ectasian period.

250 **5. Discussion**

251 **5.1. The connections between South America–South Africa margins**

252 The connections between East South America and West African margins have been
 253 known since du Toit (1927), and hundreds of research studies improved this knowledge
 254 throughout the last century (e.g., Selton et al., 2012; Blaich et al., 2013). Nevertheless, despite
 255 these efforts, certain geological gaps remain open. Since the development of GPlates Software
 256 (Müller et al., 2018), the representation of plate tectonic positions and motions has been
 257 substantially improved. In South America and Africa, the stretching process begins at 155 Ma
 258 in the southernmost portion, southward of the study area (Jokat et al., 2003). Using this as a
 259 time constraint and based on the rotational poles from Müller et al. (2019), we reconstructed
 260 the pre-to-early stretching process before oceanic crust formation at 150 Ma (Fig. 5). The
 261 reconstruction incorporating the magnetic and gravimetric data to the block models allowed us
 262 to establish the lack of a clear structure connection between the margins. The lack of direct
 263 correlation between structures on opposing margins raises significant questions about the

264 amount of crustal loss during the continental break-up process. This discrepancy suggests that
265 our current understanding of crustal evolution during rifting may be incomplete or
266 oversimplified. This apparent disconnect could indicate limitations in the current
267 reconstruction modeling approaches. They may incorrectly extrapolate features across the
268 margins or fail to capture the full complexity of the breakup process.

269 The structural features of the conjugate margins of southern South America and Africa
270 present distinct orientations that suggest these margins were not perfectly aligned prior to the
271 opening of the South Atlantic. While the fabric of southern South America strikes NE–SW, the
272 structural trend of the African counterpart strikes E–W (Fig. 5). This divergence in structural
273 fabric indicates that the connection between both margins was located in a geotectonic
274 boundary among blocks with different geological histories. A similar setting has been described
275 for the conjugate margins of North America, where a collapse of the Caledonian orogenic belt
276 preceded the formation of the North Atlantic Ocean (Schiffer et al., 2020). This orogenic
277 collapse may have also occurred between southern South America and Africa during the initial
278 stages of the rifting of SW Gondwana, which led to the development of the South Atlantic
279 Ocean basin. This scenario is quite different from the São Francisco-Congo cratons, which
280 were rifted inside the cratonic area where the geology of both margins reflects a more
281 continuous structure (Heilbron et al., 2016). In the South Brazil/Namibia conjugate margin, the
282 geology does not show an obvious geological correlation and indicates that the Atlantic margin
283 was locally formed in an orogenic belt zone between cratons. The major Precambrian structures
284 strongly controlled the South Atlantic opening, so it has the same structural orientation as the
285 Pan-African/Brasiliano belt. These inherited structures might be worked as the main conduit
286 of the SDR magmatism (Serratt et al., 2022) as well controlled the LIP volcanism and dyke
287 orientation (Tomazzoli et al., 2008; Gomes Vasconcelos, 2021). In this way, the inherited
288 structures are a weak zone in the lithosphere and should make a quick break-up with adiabatic
289 mantle decompression.

290 **5.2. Recognizing the stretched crust**

291 The clues for the lack of a direct connection between these two continents begin to be
292 clear when we interpret the seismic lines from both margins. A hyperextended continental crust
293 occurs below a thick volcanic and sedimentary package of Cretaceous to recent rocks (Figs. 2
294 and 3; Chauvet et al., 2021). However, determining oceanic and continental crust boundaries
295 in volcanic passive margins is challenging. It involves significant uncertainties and
296 subjectivity, leading to varying estimates of its location by 100–200 km or more across
297 different studies focusing on the same margin (Eagles et al., 2015). These discrepancies arise
298 from the limitations in geophysical data resolution and differences in data interpretation
299 methodologies. For instance, features such as SDR or a high-velocity lower crust pose
300 challenges, as they can be interpreted as either altered continental crust or igneous oceanic
301 crust.

302 Additionally, the interpretation of gravity data introduces non-uniqueness, with the
303 uncertainty in continental-oceanic boundary (COB) location often exceeding 100 km (Eagles
304 et al., 2015). Linear gravity lows produced by oceanic fracture zones offer valuable indicators
305 of the seaward extent of oceanic crust, but they are sporadic features, providing an intermittent
306 COB estimate. Also, according to early models, oceanic-type accretion generates pairs of linear
307 magnetic anomalies, indicators of oceanic crust, and can be related to isochrons formed by
308 seafloor spreading. However, seaward-dipping reflectors at conjugate volcanic passive margins
309 also produce linear magnetic anomalies (Geoffrey et al., 2022). Consequently, identifying an

310 accurate COB remains challenging, underscoring the need for caution when utilizing COB
311 estimates for reconstructions or plate kinematic modeling.

312 Considering this background, we utilized the previously documented magnetic
313 anomalies M2 and M4 (Rabinowitz and Labrecque, 1979; Moulin et al., 2010) as tools to
314 delineate these boundaries. The initial rifting phase occurred between the M4 and M2 chrons,
315 with the magnetic anomaly M2 indicating the onset of oceanic crust formation (Koopmann et
316 al., 2014; Fig. 3). This early stage was marked by the flexure of the basement and the extrusion
317 of proximal Seaward Dipping Reflectors (SDRs), which caused pronounced magnetic
318 anomalies (Serratt et al., 2022). Drawing on these findings, we were able to estimate the extent
319 of continental crust, which spans up to 350 km beneath the volcanic and sedimentary layers of
320 the passive margin basins along the conjugate margins in southern Brazil/Uruguay and
321 Namibia/South Africa.

322 Restoring the crust involves a 125–250 km continental crust section covered by
323 volcanic and sedimentary rocks in the Pelotas, Punta del Este, Walvis, Luderitz, and Orange
324 basins. However, it is important to note that the methodology assumes that the bulk extension
325 in the margin is pure shear, which is not always the case. One way to address the issue is by
326 estimating lower-bound values of horizontal extension rates. This can be achieved by dating
327 pairs of cross-cutting pre-flexure and post-flexure dykes, as done in eastern Greenland (Lenoir
328 et al., 2003). Another challenge is the emplacement of dykes in the margins. In a volcanic
329 passive margin, the volume of dykes can exceed 50% (Myers, 1980). Therefore, the restored
330 section will be 50% smaller, with a real extension of continental crust reaching 125 to 250 km
331 in length. This estimative is almost the most conservative scenario and does not consider the
332 denudation that occurred in these sections; even in this more conservative scenario, the impacts
333 of this in the geotectonic models and the understanding of the geology of this region are critical
334 and have not been considered previously.

335 **5.3. SW Africa, SE Brazil, and Uruguay geological correlation challenges**

336 South America and Africa were amalgamated throughout the Pan-African/Brasiliano
337 tectonic cycle along the Neoproterozoic (Caxito et al., 2021). The comparison of U-Pb data from
338 both margins can yield valuable insights into the crustal growth history and the main geological
339 events that have shaped the region (Gehrels, 2014; Roberts and Spencer, 2015) and how this
340 crustal growth history is different on both sides of South Atlantic crustal margins (Figs. 2 and
341 4). Although both margins shared the same Cryogenian to Ediacaran age peak, recording the
342 continental docking during the Gondwana supercontinent amalgamation, which was less
343 represented on the African side but still occurring, the older basement history is almost entirely
344 different. The U-Pb zircon age distribution patterns in SW Africa show major peaks at Archean,
345 Orosirian, and Stennian. Conversely, southern Brazil–Uruguay shows dominant peaks at
346 Rhyacian and Tonian, revealing their distinct crustal growth history. It is clear that both
347 margins, which were merged during the Gondwana supercontinent amalgamation, have
348 previously undergone different crustal evolutions. This distinct crustal growth record is
349 associated with the lack of continuity in the geological structures, and the identified stretched
350 crust well demonstrates the geological significance of this section in correlation studies.

351 In trying to provide a geological model of the Neoproterozoic orogenic belts of this
352 region, several authors proposed different models (e.g., Chemale, 2000; Basei et al., 2008;
353 Konopásek et al., 2020). Most proposed models do not consider the unknown stretched
354 continental crust under the passive margin basin. Here, through GPlates reconstruction and
355 deep seismic profiles analysis presented by Chauvet et al. (2021) along both margins, we point

356 out that the lithosphere stretching estimated the missing of at least 150–300 linear km of
357 continental crust that is hyperextended beneath the Punta del Este (Uruguay), Pelotas (southern
358 Brazil) and Orange, Luderitz, Namibia, and Walvis basins (southwest Africa). This result
359 indicates that a significant portion of the Pan-African/Brasiliano orogenic belt and its
360 underlying basement is missing. The present size of the Dom Feliciano Belt, which is the
361 expression of Pan-African/Brasiliano orogeny in southernmost Brazil and Uruguay, is smaller
362 than this. This missing continental crust section is comparable in size to the main sections of
363 the Andean, Rocky, or Ural mountains.

364 This unknown stretched crust, comparable in size to the Earth's largest orogens and covered
365 by Cretaceous rocks of the passive margins, must be considered in any paleogeographic and
366 geotectonic model that intends to evaluate the connection of Pan-African/Brasiliano belts. The
367 question is, what is the nature of this continental crust? May we speculate that the missing
368 puzzle of the Pan-African/Brasiliano petroTECTONIC assemblages can be there, such as juvenile
369 Ediacaran island and magmatic arcs, ophiolite slabs of the Adamastor Ocean, and others? Is it
370 possible to have a more robust idea of the direction of the subduction paleo plates?

371 These questions remain largely unanswered, posing significant challenges to many
372 proposed geotectonic models without considering the existence of extended continental crust
373 covered by thick volcanic and sedimentary layers in passive margin tectonic settings. This
374 oversight includes the previously unrecognized stretched continental crust in the Atlantic
375 Ocean, which is the physical extension of the Neoproterozoic to Eopaleozoic Dom Feliciano,
376 Saldania, Gariep, and Kaoko belts (e.g., Porada, 1989; Rapela et al., 2011; Konopásek et al.,
377 2020). The 150–300 km gap in the continental crust harbors key petroTECTONIC assemblages
378 essential for understanding the processes by which these terranes were amalgamated. However,
379 our understanding of the composition and characteristics of these assemblages remains
380 incomplete. Even with the development of plausible tectonic models, critical puzzle pieces
381 concerning mobile belts exposed in the emerged sections of the conjugate margins will often
382 remain speculative.

383 **6. Conclusion**

384 This study enhanced our approach to understanding the conjugate margins of the South
385 Atlantic Ocean, bringing new insights into pre-rifting geological terrain assemblage models of
386 Pangea and SW Gondwana. The geophysical anomalies, seismic interpretations, and U-Pb
387 isotopic data contribute to a nuanced understanding of the geological evolution in the
388 southwestern Gondwana supercontinent, delineating the extent of the stretched crust and now
389 concealed beneath passive margin basins. However, they are insufficient for precisely
390 determining this extended crust's nature and composition for further geological correlation of
391 the SW Gondwana supercontinent. The integration of paleo reconstruction models with
392 offshore seismic interpretation profiles of hyperextended margins has revealed the inherent
393 limitations of directly reconstructing and connecting geological terranes across different
394 margins, such as those of southeastern South America and southwestern Africa. Consequently,
395 current paleogeographic reconstructions and the associated geological models for the emerging
396 continental margins of the South Atlantic lack the accuracy to account for the extensive and
397 concealed hyperextended crust. After restoring the hyperextended crust, these previous
398 reconstruction models fail to account for a substantial portion of the continental crust, estimated
399 to be at least 150–300 km. This study significantly advances our knowledge of hyperextended
400 passive margins and contributes to a more realistic portrayal of Precambrian terrane evolution.

401 **Acknowledgments**

402 This study was supported by the UNISINOS-PETROBRAS and UNISINOS-CNODC
403 Cooperation Agreements. We also thank the National Administration of Fuels, Alcohols, and
404 Portland (ANCAP) and the Brazilian National Agency for Petroleum, Natural Gas, and
405 Biofuels (ANP) for providing data access. We are grateful to Sequent and Eliis for granting
406 academic licenses for the Oasis Montaj and PaleoScan™ software, respectively. FCJ
407 acknowledges the Brazilian National Council for Scientific and Technological Development
408 (CNPq) for grant #408194/2021-9. We are particularly grateful to Bruce Eglinton, Dengliang
409 Gao, and an anonymous reviewer for their insightful comments. Finally, we acknowledge
410 editors M. Santosh and Richard Damian Nance for their efforts in handling the publication of
411 this manuscript.

412 **References**

- 413 Basei, M.A.S., Frimmel, H.E., Nutman, A.P., Preciozzi, F., 2008. West Gondwana
414 amalgamation based on detrital zircon ages from Neoproterozoic Ribeira and Dom Feliciano
415 belts of South America and comparison with coeval sequences from SW Africa. *Geological*
416 *Society, London, Special Publications* 294(1), 239-256.
- 417 Becker-Kerber, B., Paim, P.S.G., Junior, F.C., et al., 2020. The oldest record of
418 Ediacaran macrofossils in Gondwana (~ 563 Ma, Itajaí Basin, Brazil). *Gondwana Res.* 84, 211-
419 228.
- 420 Begg, G.C., Griffin, W.L., Natapov, L.M., et al., 2009. The lithospheric architecture of
421 Africa: Seismic tomography, mantle petrology, and tectonic evolution. *Geosphere* 5(1), 23-50.
- 422 Blaich, O.A., Faleide, J.I., Tsikalas, F., Gordon, A.C., Mohriak, W., 2013. Crustal-scale
423 architecture and segmentation of the South Atlantic volcanic margin. *Geological Society,*
424 *London, Special Publications* 369(1), 167-183.
- 425 Caxito, F.A., Hartmann, L.A., Heilbron, M., Bruno, H., Pedrosa-Soares, A., Basei,
426 M.A.S., Chemale, F., 2022. Multi-proxy evidence for subduction of the Neoproterozoic
427 Adamastor Ocean and Wilson cycle tectonics in the South Atlantic Brasiliano Orogenic
428 System of Western Gondwana. *Precambrian Res.* 376, 106678
- 429 Chauvet, F., Sapin, F., Geoffroy, L., Ringenbach, J.C., Ferry, J.N., 2021. Conjugate
430 volcanic passive margins in the austral segment of the South Atlantic—Architecture and
431 development. *Earth-Sci. Rev.* 212, 103461.
- 432 Chemale Jr, F., 2000. Evolução geológica do Escudo Sul-rio-grandense. *Geologia do*
433 *Rio Grande do Sul*, 13-52.
- 434 Chemale Jr, F., Mallmann, G., de Fátima Bitencourt, M., Kawashita, K., 2012. Time
435 constraints on magmatism along the Major Gercino Shear Zone, southern Brazil: implications
436 for West Gondwana reconstruction. *Gondwana Res.* 22(1), 184-199.
- 437 Doré, T., Lundin, E., 2015. Research focus: Hyperextended continental margins—
438 Knowns and unknowns. *Geology* 43(1), 95-96.

- 439 Du Toit, A.L., 1927. A geological comparison of South America with South Africa (No.
440 381). Carnegie Institution of Washington.
- 441 Eagles, G., Pérez-Díaz, L., Scarselli, N., 2015. Getting over continent ocean boundaries.
442 Earth-Sci. Rev. 151, 244-265.
- 443 Fernandes, L.A.D., Tommasi, A., Porcher, C.C., 1992. Deformation patterns in the
444 southern Brazilian branch of the Dom Feliciano Belt: A reappraisal. J. South Am. Earth Sci.
445 5(1), 77–96. doi:10.1016/0895-9811(92)90061-3.
- 446 Frimmel, H.E., 2009. Trace element distribution in Neoproterozoic carbonates as
447 palaeoenvironmental indicator. Chem. Geol. 258(3-4), 338-353.
- 448 Gehrels, G., 2014. Detrital Zircon U-Pb Geochronology Applied to Tectonics. An. Rev.
449 Earth Planet. Sci. 42, 127-149
- 450 Gomes, A.S., Vasconcelos, P.M., 2021. Geochronology of the Paraná-Etendeka large
451 igneous province. Earth-Sci. Rev. 220, 103716.
- 452 Heilbron, M., Cordani, U.G., Alkmim, F.F. (Eds.), 2016. Sao Francisco Craton, Eastern
453 Brazil: Tectonic Genealogy of a Miniature Continent. Springer.
- 454 Heine, C., Zoethout, J., Müller, R.D., 2013. Kinematics of the South Atlantic rift. Solid
455 Earth 4(2), 215-253.
- 456 Jokat, W., Boebel, T., König, M., Meyer, U., 2003. Timing and geometry of early
457 Gondwana break-up. J. Geophys. Res.: Solid Earth 108(B9).
- 458 Konopásek, J., Cavalcante, C., Fossen, H., Janoušek, V., 2020. Adamastor – an ocean
459 that never existed? Earth-Sci. Rev. 205, 103201.
460 <https://doi.org/10.1016/j.earscirev.2020.103201>
- 461 Koopmann, H., Schreckenberger, B., Franke, D., Becker, K., Schnabel, M., 2014. The
462 late rifting phase and continental break-up of the southern South Atlantic: the mode and timing
463 of volcanic rifting and formation of earliest oceanic crust. Geological Society, London, Special
464 Publications 420(1), 315-340.
- 465 Lei, C., Alves, T. M., Ren, J., Tong, C., 2020. Rift structure and sediment infill of
466 hyperextended continental crust: insights from 3D seismic and well data (Xisha Trough, South
467 China Sea). J. Geophys. Res.: Solid Earth 125(5), e2019JB018610.
- 468 Lenoir, X., Féraud, G., Geoffroy, L., 2003. High-rate flexure of the East Greenland
469 volcanic margin: constraints from $^{40}\text{Ar}/^{39}\text{Ar}$ dating of basaltic dykes. Earth Planet. Sci. Lett.
470 214(3-4), 515-528.
- 471 Macdonald, D., Gomez-Perez, I., Franzese, J., et al., 2003. Mesozoic break-up of SW
472 Gondwana: implications for regional hydrocarbon potential of the southern South Atlantic.
473 Marine and Petroleum Geology 20(3-4), 287-308.
- 474 Maus, S., Barckhausen, U., Berkenbosch, H., et al., 2009. EMAG2: A 2-arc min
475 resolution Earth Magnetic Anomaly Grid compiled from satellite, airborne, and marine
476 magnetic measurements. Geochem. Geophys. Geosys. 10(8).

- 477 McKenzie, D., 1978. Some remarks on the development of sedimentary basins. *Earth*
478 *Planet. Sci. Lett.* 40(1), 25–32. doi:10.1016/0012-821x(78)90071-7
- 479 Milani, E.J., De Wit, M.J., 2008. Correlations between the classic Paraná and Cape–
480 Karoo sequences of South America and southern Africa and their basin infills flanking the
481 Gondwanides: du Toit revisited. *Geological Society, London, Special Publications* 294(1),
482 319-342.
- 483 Miller, R., Grote, W., 1988. Geological Map of the Damara Orogen, South West
484 Africa/Namibia 1: 500 000. Geological Survey.
- 485 Moulin, M., Aslanian, D., Unternehr, P., 2010. A new starting point for the South and
486 Equatorial Atlantic Ocean. *Earth-Sci. Rev.* 98(1-2), 1–37. doi:10.1016/j.earscirev.2009.08.001
- 487 Müller, R.D., Zahirovic, S., Williams, S.E., et al., 2019. A global plate model including
488 lithospheric deformation along major rifts and orogens since the Triassic. *Tectonics* 38(6),
489 1884-1907.
- 490 Müller, R.D., Cannon, J., Qin, X., et al., 2018. GPlates: building a virtual Earth through
491 deep time. *Geochem. Geophys. Geosyst.* 19. <https://doi.org/10.1029/2018GC007584>.
- 492 Mutter, J.C., Talwani, M., Stoffa, P.L., 1982. Origin of seaward-dipping reflectors in
493 oceanic crust off the Norwegian margin by "subaerial seafloor spreading". *Geology* 10(7), 353-
494 357.
- 495 Myers, J.S., 1980. Structure of the coastal dyke swarm and associated plutonic
496 intrusions of East Greenland. *Earth Planet. Sci. Lett.* 46(3), 407-418.
- 497 Nirrengarten, M., Manatschal, G., Tugend, J., Kusznir, N., Sauter, D., 2018. Kinematic
498 evolution of the southern North Atlantic: Implications for the formation of hyperextended rift
499 systems. *Tectonics* 37, 89–118. <https://doi.org/10.1002/2017TC004495>.
- 500 Passchier, C.W., Trouw, R.A.J., Ribeiro, A., Paciullo, F.V.P., 2002. Tectonic evolution
501 of the southern Kaoko belt, Namibia. *J. Afr. Earth Sci.* 35(1), 61-75.
- 502 Peron-Pinvidic, G., Manatschal, G., Osmundsen, P.T., 2013. Structural comparison of
503 archetypal Atlantic rifted margins: A review of observations and concepts. *Marine and*
504 *Petroleum Geology* 43, 21-47.
- 505 Porada, H., 1989. Pan-African rifting and orogenesis in southern to equatorial Africa
506 and eastern Brazil. *Precambrian Res.* 44(2), 103-136.
- 507 Prave, A.R., 1996. Tale of three cratons: Tectonostratigraphic anatomy of the Damara
508 orogen in northwestern Namibia and the assembly of Gondwana. *Geology* 24(12), 1115-1118.
- 509 Puetz, S.J., Spencer, C.J., Ganade, C.E., 2021. Analyses from a validated global U-Pb
510 detrital zircon database: Enhanced methods for filtering discordant U-Pb zircon analyses and
511 optimizing crystallization age estimates. *Earth-Sci. Rev.* 220, 103745.
- 512 Rabinowitz, P.D., LaBrecque, J., 1979. The Mesozoic South Atlantic Ocean and
513 evolution of its continental margins. *J. Geophys. Res.* 84(B11), 5973.
514 doi:10.1029/jb084ib11p05973

- 515 Rapela C.W., Fanning C.M., Casquet C., Pankhurst R.J., Spalletti L., Poiré D., Baldo
516 E.G., 2011. The Rio de la Plata craton and the adjoining Pan-African/Brasiliano terranes: Their
517 origins and incorporation into southwest Gondwana. *Gondwana Res.* 20, 673-690.
- 518 Roberts, N.M.W., Spencer, C.J., 2015. The zircon archive of continent formation
519 through time. In: Roberts, N.M.W., Van Kranendonk, M., Parman, S., Shirey, S., Clift, P.D.
520 (Eds.), *Continent Formation Through Time*. Geological Society, London, Special Publications,
521 389, 197 – 225.
- 522 Salomon, E., Passchier, C., Koehn, D., 2017. Asymmetric continental deformation
523 during South Atlantic rifting along southern Brazil and Namibia. *Gondwana Res.* 51, 170-176.
- 524 Sandwell, D.T., Müller, R.D., Smith, W.H.F., Garcia, E., Francis, R., 2014. New global
525 marine gravity model from Cryo-Sat-2 and Jason-1 reveals buried tectonic structure. *Science*
526 346(6205), 65-67. doi: 10.1126/science.1258213.
- 527 Schiffer, C., Doré, A.G., Foulger, G.R., et al., 2020. Structural inheritance in the North
528 Atlantic. *Earth-Sci. Rev.* 206, 102975.
- 529 Serratt, H., Teixeira, C.D., Girelli, T.J., Kehl de Souza, M., Vargas, M.R., Silva, A.M.,
530 Chemale Jr, F., 2022. Seaward-dipping reflector influence on seafloor magnetostratigraphy—A
531 Pelotas Basin view. *Geophys. Res. Lett.* e2022GL100382.
- 532 Seton, M., Müller, R.D., Zahirovic, S., et al., 2012. Global continental and ocean basin
533 reconstructions since 200 Ma. *Earth-Sci. Rev.* 113(3-4), 212-270.
- 534 Sutra, E., Manatschal, G., Mohn, G., Unternehr, P., 2013. Quantification and restoration
535 of extensional deformation along the Western Iberia and Newfoundland rifted margins.
536 *Geochem. Geophys. Geosyst.* 14, 2575–2597. doi:10.1002/ ggge.20135.
- 537 Torsvik, T.H., Rouse, S., Labails, C., Smethurst, M.A., 2009. A new scheme for the
538 opening of the South Atlantic Ocean and the dissection of an Aptian salt basin. *Geophys. J. Int.*
539 177(3), 1315-1333.
- 540 Veevers, J.J., 2004. Gondwanaland from 650–500 Ma assembly through 320 Ma
541 merger in Pangea to 185–100 Ma break-up: supercontinental tectonics via stratigraphy and
542 radiometric dating. *Earth-Sci. Rev.* 68(1-2), 1-132.
- 543 Vermeesch, P., 2018. IsoplotR: A free and open toolbox for geochronology. *Geosci.*
544 *Front.* 9(5), 1479-1493.

546 **Figures and table captions**

547 Fig. 1. (a) Distribution of main cratons in the West Gondwana context. WA–West Africa
 548 Craton; AM–Amazonian Craton, SF–São Francisco Craton; CO–Congo Craton; K–Kahalari
 549 Craton; RP–Rio de la Plata Craton; (b) detailed view of main Brasiliano/PanAfrican belts and
 550 surroundings cratonic areas. DFB–Dom Feliciano Belt; KB–Kaoko Belt; DB–Damara Belt;
 551 GB–Gariep Belt; SB–Saldanha Belt (after Becker-Kerber et al., 2020).

552 Fig. 2. Seismic profiles b–b' and well data across the conjugate margins of the northern Pelotas
 553 (a) and Lüderitz (b) basins (Fig. 3). Well 2-BPS-6A, located in the Pelotas Basin, sampled
 554 volcanic units inserted in (a). The Lüderitz Basin profile (b) was adapted from Chauvet et al.
 555 (2021).

556 Fig. 3. (a) Sketch of SW Gondwana map reconstructed at 118 Ma according to the global plate
 557 model that includes plate deformation along major rifts and orogens of Müller et al. (2019),
 558 with the position of studies seismic profiles; background data: topography SRTM1 grid. The
 559 red areas correspond to the outcropping of Brasiliano/Pan-African terranes in the SW
 560 Gondwana. The top right inset with South America and Africa maps is 118 Ma. 2D seismic
 561 interpretation profiles are modified from Chauvet et al. (2021): (b and b') above: gravimetry
 562 and magnetic profiles; below: schematic interpretation seismic profiles b and b'; and (c and c')
 563 above: gravimetry and magnetic profiles; below: schematic interpretation seismic profiles c
 564 and c'. The gray line on the magnetic profile shows magnetic anomaly from Rabinowitz and
 565 Labrecque (1979) and Moulin et al. (2010). The darker red lines in the profiles mark the
 566 boundary of the upper and lower continental crust. The crustal stretching factor (β) is calculated
 567 along the stretched crust with regular spacing (black dashed vertical line). The boundary
 568 between the hyperextended continental crust and oceanic crust (dark blue) is unclear in seismic
 569 interpretations. Basins: NB – Namibia; SB – Santos; WB – Walvis; LB – Luderitz; PB –
 570 Pelotas; PLB – Punta del Este; OB – Orange; SLB – Salado; and CB – Colorado.

571 Fig. 4. U-Pb zircon data from Southeastern South America, encompassing southeast Brazil,
 572 Uruguay, and SW Africa (Pan-African Belts). The U-Pb data were plotted using IsoplotR
 573 online (Vermeesch, 2018).

574 Fig. 5. Sketch of SW Gondwana map reconstructed according to the global plate model of
 575 Müller et al. (2019) showing the lack of connection between the structures of South America
 576 and African margins. White line: Large Magnetic Anomaly. Reconstructions use (a) the Earth
 577 Magnetic Anomaly Model from Maus et al. (2009) and (b) Satellite Free-air Gravity Anomaly
 578 data from Sandwell et al. (2014). Basins: NB – Namibia; SB – Santos; WB – Walvis; LB –
 579 Luderitz; PB – Pelotas; PLB – Punta del Este; OB – Orange; SLB – Salado; and CB – Colorado.

580 **Table 1** UCC: Unstretched Continental Crust; SCC: Stretched Continental Crust; β : stretching
 581 factor, magnitude of the extension; a Unstretched crust for sections b–b' and c–c'; b stretched
 582 restored crust considering 50% of volcanic dikes; c stretched restored crust considering 50%
 583 of volcanic dikes for sections b–b' and c–c'; d final gap: sum of unstretched and restored crust
 584 for both sections.

585 • A multi-tool approach reveals at least 150 km of hyperextended continental crust.

586

587 • This study highlights the significance of stretching in reconstruction studies.

588

589
590
591
592
593
594
595

- Distinct U-Pb zircon age distribution patterns reinforce the lack of direct connections.
- New insights on the dynamics of hyperextended crust.
- A significant portion of the Brazilian/Pan-African orogenic belt is hidden beneath passive margin basins.

Journal Pre-proofs

Figure 1

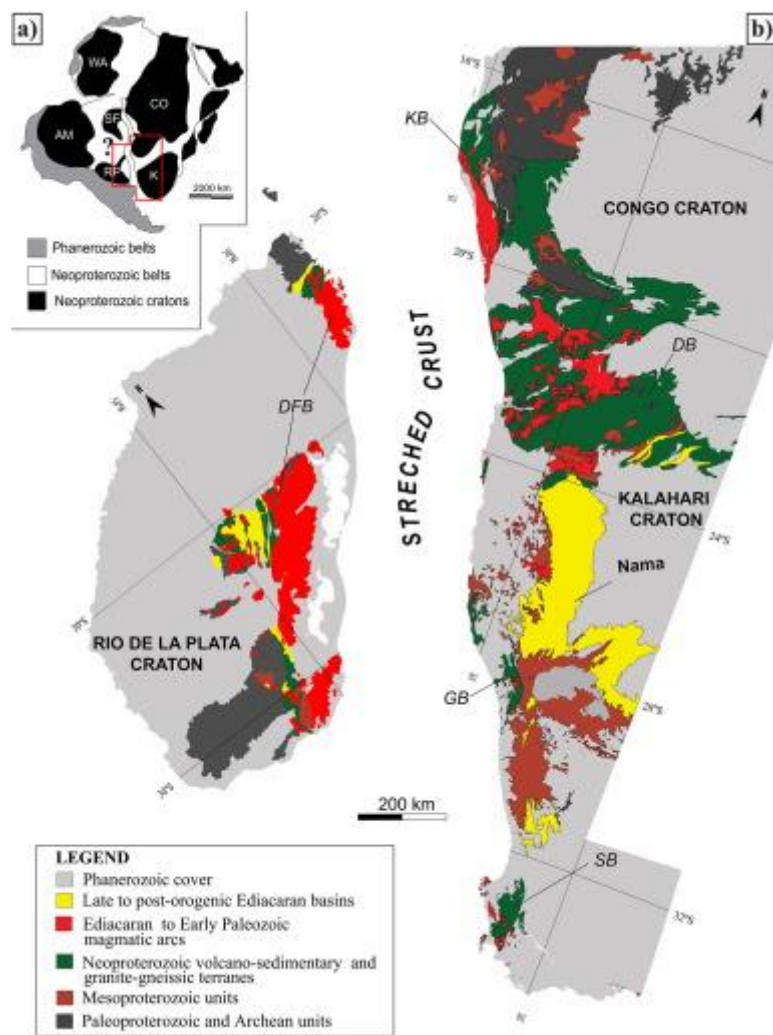


Figure 2

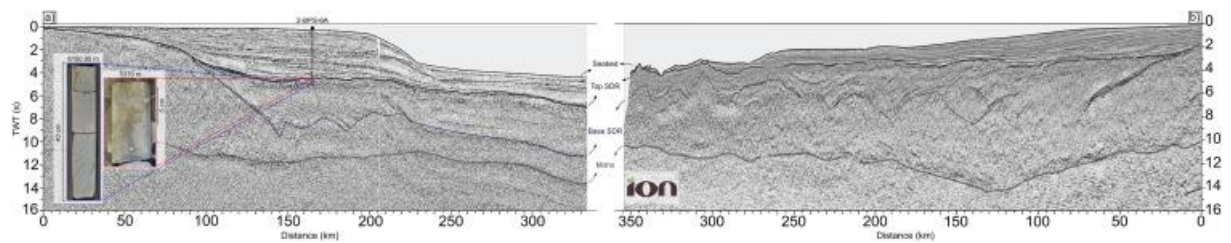


Figure 3

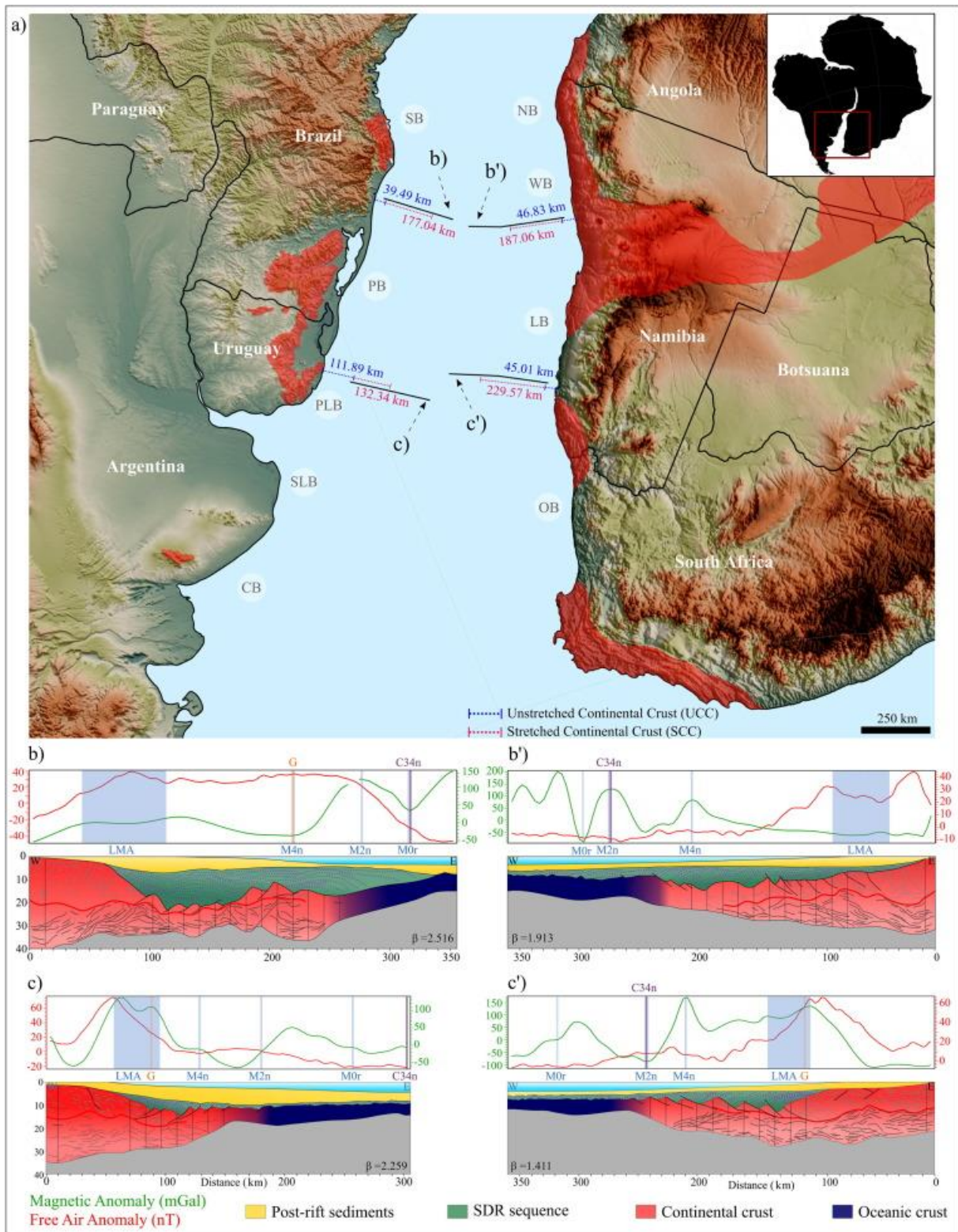


Figure 4

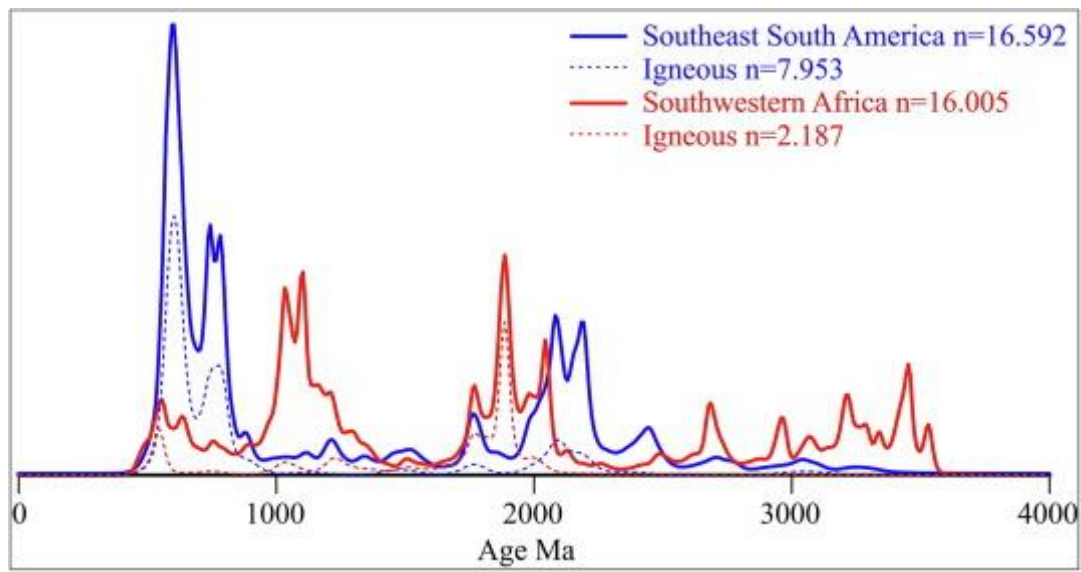


Figure 5

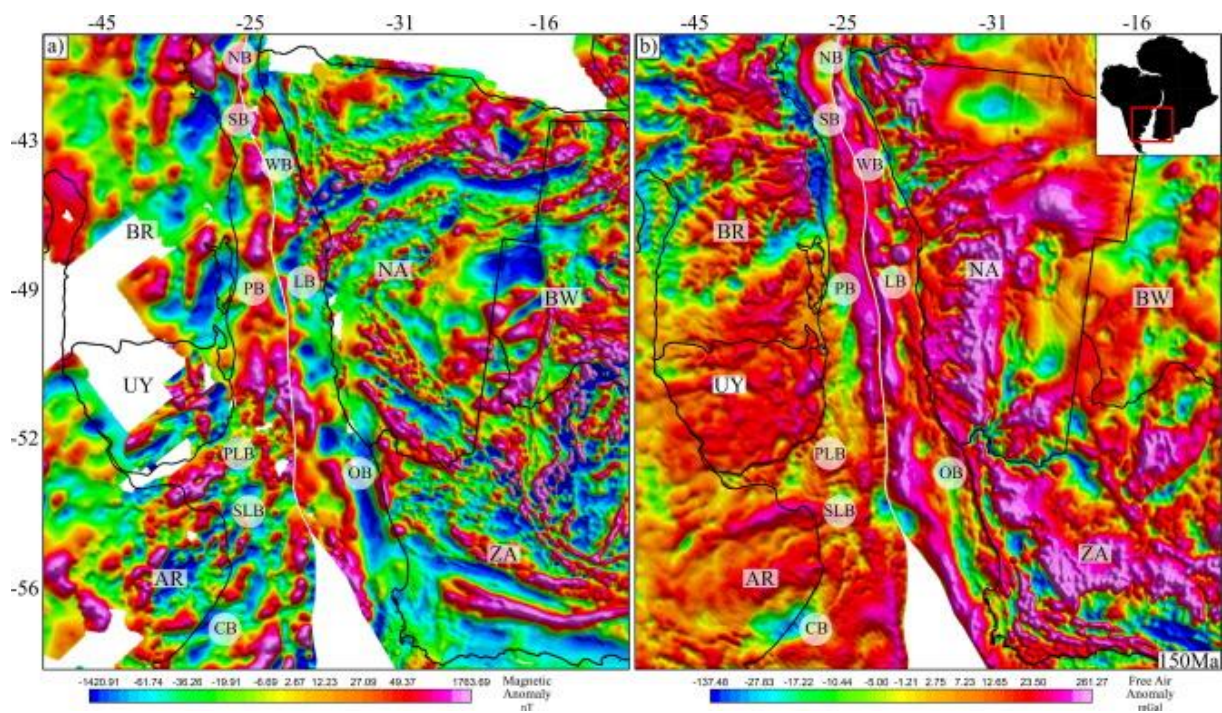


Table 1

Section	CCU	CCS	β	Stretched	Stretched 50 % ^a	Restored ^b	Unstretched ^c	Stretched 50 % ^d	Gap ^e
Northern Pelotas and Walvis basins (Section B-B')									
B	39.49	177.04	2.52	70.3656598	35.18	74.68	86.33	84.07	170.40
B'	46.83	187.06	1.91	97.783586	48.89	95.72			
Punta del Este and Lüdertiz basins (Section C-C')									
C	111.90	132.35	2.26	58.5878707	29.29	141.19	156.92	110.64	267.56
C'	45.02	229.57	1.41	162.700213	81.35	126.37			